Korean J. Chem. Eng., 40(11), 2657-2670 (2023)
DOI: 10.1007/s11814-023-1520-1

pISSN: 0256-1115
eISSN: 1975-7220

Techno-economic analysis of green and blue hybrid processes for ammonia production

Sungjun Park, Yonghyeon Shin, Eunha Jeong, and Myungwan Han†

Department of Chemical Engineering & Applied Chemistry, Chungnam National University,
99 Daehak-ro, Yuseong-gu, Daejeon 34134, Korea
(*Received 9 February 2023 • Revised 17 June 2023 • Accepted 29 June 2023*)

Abstract−In a blue ammonia plant, hydrogen required for ammonia synthesis is traditionally produced through steam reforming. This process is cost competitive but has the drawbacks of high CO_2 emissions and excessive energy consumption. On the other hand, in a green ammonia plant, hydrogen production through water electrolysis avoids CO_2 emissions and utilizes renewable energy sources. However, high stack costs and electricity prices degrades the economic viability of the process. Recognizing the potential benefits of both green and blue ammonia production methods, novel hybrid processes have been proposed to integrate these approaches. A thermoneutral tri-reformer has been introduced as a replacement for the energy-intensive steam reforming process, offering a means to eliminate CO_2 emissions. In the green ammonia process, hydrogen generated by a water electrolyzer, along with nitrogen obtained from an air separation unit (ASU), are employed for ammonia synthesis. However, the high-purity oxygen produced as a byproduct from the electrolyzer and ASU has not been utilized thus far. This oxygen can be fed into the tri-reformer to produce blue hydrogen or syngas. To evaluate the technical and economic advantages resulting from the integration of these systems, a techno-economic assessment was conducted on these hybrid processes as well as conventional ones in the literature [3]. The results demonstrate that the proposed processes exhibit superior economic performance compared to conventional approaches, highlighting the potential benefits of system integration.

Keywords: Hybrid Process, Ammonia Synthesis, Green Ammonia, Blue Ammonia, Syngas, Technoeconomic Analysis

INTRODUCTION

Ammonia is one of the largely produced industrial chemicals, mainly used for producing fertilizer, explosives, fibers, plastics. Global production rate of ammonia was 235 million tons in 2019 [1]. Recently, ammonia has been focused as a carbon-free energy carrier due to its intrinsic merits in terms of storage and transportation compared with hydrogen [2]. Ammonia production is predominantly reliant on natural gas, leading to significant CO_2 emissions released into the atmosphere. The industrial synthesis of ammonia involves processes such as steam reforming of natural gas, autothermal reforming, and the Harber-Borsch (H-B) process [3]. The steam reforming of natural gas, which provides hydrogen for subsequent use in the H-B processes, is highly energy intensive due to its highly endothermic nature. Ammonia derived from natural gas is commonly referred to as "blue ammonia". Notably, the H-B process accounts for approximately 1-2% of global energy consumption and contributes to around 1.2% of global CO_2 emissions [4]. This makes the blue ammonia process one of the largest energy consumers and greenhouse gas emitters. While the nitrogen used in the process is sourced from ambient air, the production of hydrogen requires the most substantial energy input. Consequently, the cost-effective production of clean hydrogen poses a significant challenge for the production of low-cost, environmentally friendly ammonia [5]. Presently, 45% of pure hydrogen production from natural gas is utilized for ammonia synthesis. It is very important to prioritize green hydrogen production to mitigate fossil fuel consumption and greenhouse gas emissions.

Green ammonia production processes that utilize green hydrogen need to be investigated. Biomass gasification and water electrolysis powered by renewable energy offer promising solutions to produce green hydrogen. Biomass gasification produces a mixture of H_2, CO and CO_2, which undergoes several processing stages to yield high-purity hydrogen. A substantial air separation unit (ASU) is necessary to supply oxygen for the gasification process and the byproduct (nitrogen) can be utilized for ammonia synthesis. However, it is important to note that the installation of gasification and air separation units requires a large investment, and energy efficiency of the overall process is relatively low [4,6,7].

Water electrolysis produces carbon-free hydrogen. The electrolyzer splits water into hydrogen and oxygen electrochemically. The process can be coupled with the H-B process to produce ammonia without the use of fossil fuels [8]. High temperature solid-oxide electrolysis (SOE) is more suitable for coupling with the ammonia synthesis process than other low-temperature electrolysis technologies, alkaline electrolysis and polymer electrolyte membrane electrolysis [9]. This is due to two main factors: (1) higher electrical efficiency achieved at temperatures above 650 °C through steam electrolysis, and (2) the ability to integrate heat with the ammonia synthesis process to enhance the utilization of heat at the system level. Renewable electricity from wind or solar energy can be chosen for the steam electrolysis to produce NH_3, significantly reducing greenhouse gas emissions [10]. However, SOE is still expensive, and the intermittency of renewable electricity limits the economic fea-

†To whom correspondence should be addressed.
E-mail: mwhan@cnu.ac.kr

sibility and commercialization of the process [11].

The blue ammonia process, although cost competitive compared to the green ammonia process, faces challenges due to its high energy consumption and CO_2 emissions. On the other hand, the green ammonia process is environmentally friendly but entails significant costs. Within the green ammonia process, the H-B process relies on hydrogen produced through water electrolysis and nitrogen obtained from an air separation unit (ASU) to generate ammonia. However, the high-purity oxygen, a byproduct of both electrolysis and ASU, remains unused [12]. Exploring a potential solution, integrating the green process with the blue process presents an opportunity to utilize high-purity oxygen and enhance economic performance. Tri-reforming utilizes steam, oxygen, and CO_2 in the process of methane reforming to generate syngas. This characteristic of tri-reforming enables the effective utilization of the high-purity oxygen obtained from both the electrolyzer and ASU within the green ammonia process. A novel type of thermoneutral tri-reformer, proposed by Jang and Han [13], combines endothermic and exothermic reforming reactions, eliminating the need for an external energy supply from the furnace. The tri-reformer can be used to replace conventional reforming systems, including the primary steam reformer, secondary autothermal reformer, and furnace, eliminating CO_2 emissions to atmosphere.

This study proposes three hybrid cases that integrate the blue and green ammonia processes with a tri-reformer for ammonia production. The proposed processes are investigated techno-economically and compared with convention ones. The conventional processes are methane-to-ammonia (MtA) plant, and power-to-ammonia (PtA) plant, which were studied by Zhang et al. [3]. Three new hybrid processes are MtA based on a tri-reformer (MtA-Tr) plant, MtA integrated with PtA (MtA-PtA) plant, and PtA integrated to methane-to-syngas (PtA-MtS). MtA-Tr replaces the steam reformer, furnace, and autothermal reformer in the MtA case, resulting in a reduction in capital costs. MtA-PtA introduces an electrolyzing section to produce H_2 and O_2, where H_2 can be utilized in the H-B process for NH_3 synthesis, and O_2 can be supplied to the tri-reformer for syngas (mixture of H_2 and N_2) production. PtA-MtS incorporates the PtA case and utilizes oxygen from the electrolyzer and ASU for syngas (mixture of H_2 and CO) production. In all cases, a steam turbine network (Rankine cycle) is implemented for heat recovery and electricity generation.

AMMONIA PRODUCTION SYSTEMS

1. Methane-to-ammonia (MtA)

Fig. 1 illustrates the MtA plant based on the steam methane reforming (SMR) process. The natural gas feedstock is supplied to the steam methane reformer (SMR) and the primary reformer furnace. The primary reformer furnace provides the heat required for the SMR. CO_2 is generated in the furnace during the combustion process. In the SMR, steam is also added to the reformer and steam reforming occurs. The reformed gas is mixed with a controlled amount of air and introduced to a secondary autothermal reformer, where the gas is burned and then reforming reactions take place. The H_2/N_2 mole ratio of the gas is approximately 2.5. Overall, combustion provides the energy necessary for maintaining the endo-

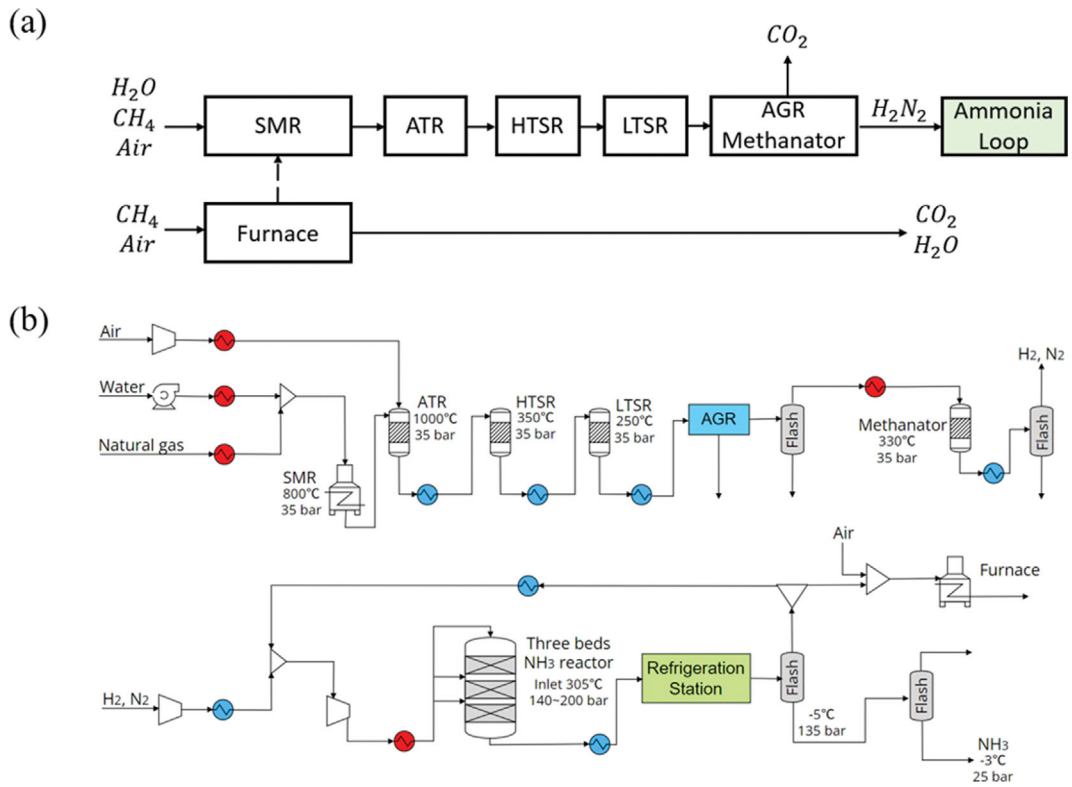

Fig. 1. Methane to ammonia process (MtA). The Rankine cycle (steam turbine network) is not shown in this figure but it is sized and optimized for maximizing heat recovery using pinch technology.

thermic reaction. The reformed syngas from the secondary reformer has a temperature of approximately 1,000 °C, and CO and H_2O in the gas are converted into H_2 and CO_2 in a high-temperature (HTSR) and low-temperature water-gas-shift reactor (LTSR). The reaction in the two reactors increases the H_2/N_2 mole ratio of the gas mixture to be 3. The CO_2 in the gas mixture is chemically absorbed and removed using monoethanol amine solvent in acid gas removal (AGR) process. Traces of CO and CO_2 are removed from the reformed gas by a methanator. The mixture of H_2 and N_2 is compressed using a multistage compressor and fed to the ammonia synthesis reactor which contains a 3-bed quench converter. After the reaction, the product gas passes through the refrigeration station and then a high-pressure and medium pressure separator to obtain pure ammonia.

2. SOE-based Power-to-ammonia (PtA)

For the case of PtA, SOE generates hydrogen and oxygen, and the air separation unit (ASU) separates air into nitrogen and oxygen. Hydrogen from SOE and nitrogen from ASU are used to produce ammonia. It follows that the hydrogen production and purification processes employed in MtA are not needed. Fig. 2 shows the block and process flow diagrams for the case of PtA. In the cathode of the SOE, demineralized water is electrolyzed to produce H_2. The product gas from the cathode travels to the flash drum where water is removed and then part of the gas is recycled to the SOE inlet to maintain the reduction atmosphere of the cathode. O_2 is produced at the anode and the O_2 produced is also partly recycled for thermal management of the stack. Hydrogen from the SOE is then mixed with the N_2 from ASU with a H_2/N_2 ratio of 3 and is fed to the ammonia synthesis loop. Oxygen from SOE and ASU is stored in an O_2 tank for sale.

3. New Processes Combining the green and Blue Ammonia Processes

The steam methane reforming reaction in MtA (the existing blue ammonia production process) is a strong endothermic reaction, so much energy must be supplied. Furthermore, the combustor in this process supplies heat to the reactor and emits carbon dioxide, which can lead to environmental problems. In terms of economics, the emission of carbon dioxide can be taken into consideration by a carbon tax.

An autothermal reformer (ATR) can be chosen for syngas generation because ATR is adiabatic and does not need a heat supply from the outside of the reactor, i.e., furnace. ATR is a technology that combines steam reforming and partial oxidation (POX). The process consists of the POX zone and subsequent steam reforming zone. The POX supplies the process heat for steam reforming. The operation temperature ranges between 900 °C and 1,500 °C. The temperature sharply increases in the exothermic region and steadily decreases in the reforming region. ATR gives a higher hydrogen yield than POX. The reactor consists of three zones: (1) the burner, where the feed streams are mixed in a turbulent diffusion flame, (2) the combustion zone producing carbon dioxide and water, and (3) the catalytic reaction zone, where steam and dry reforming take place. ATR has a high temperature in the exothermic region and a low temperature in the reforming region. The large temperature variation along the reactor makes it difficult to control the temperature of the reactor.

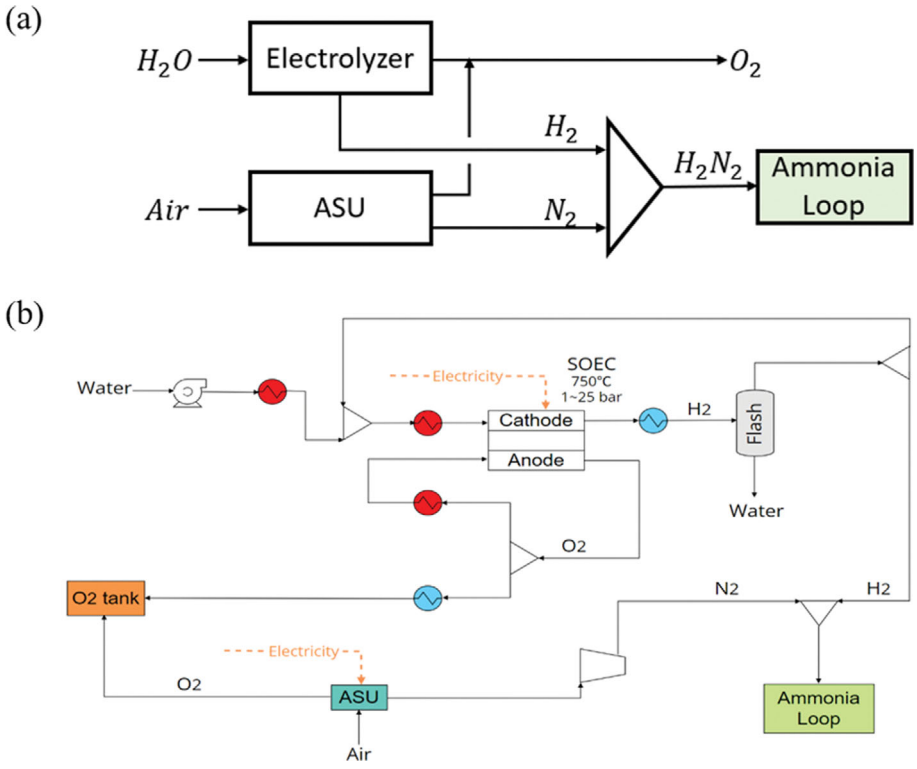

Fig. 2. Power to ammonia process (PtA). The Rankine cycle (steam turbine network) is not shown in this figure but it is sized and optimized for maximizing heat recovery using pinch technology.

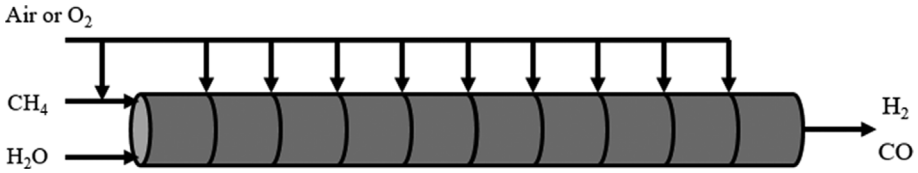

Fig. 3. Schematic diagram of the proposed tri-reformer.

Tri-reforming involves a combination of steam, dry and partial oxidation of methane. The presence of H_2O and O_2 in the reforming process mitigates carbon deposition and coke formation on the catalyst. This process can be used to produce hydrogen-rich syngas, which, consequently, improves the NH_3 production efficiency, such as reducing the production cost [12,14-17]. Tri-reforming can be employed to enhance the energy efficiency of the process [15-17]. Methane combustion can supply the energy required for reforming reactions so that external energy is not needed to proceed with the reforming reactions, increasing the energy efficiency of the process. Jang and Han [13] proposed a tri-reformer with an O_2 sidestream distribution. In some cases in this work, this structure is slightly modified to use air instead of O_2. The air side stream is distributed along the reactor to address the heat and mass management problems in the design of the tri-reformer. Nitrogen in the air supply to the tri-reformer can be directly used for ammonia production in the subsequent H-B process. Fig. 3 shows a schematic diagram of the reactor. The distributed air supply to the reactor keeps the temperature profile of the reactor within a safe temperature range and reduces the temperature gradient. This can be achieved by recovering the temperature drops due to an endothermic reaction (mainly steam reforming) by using the heat generated from the exothermic reaction (partial oxidation). This structure solves the technical problems of conventional ATR, such as reactor complexity and temperature control problems.

PtA, the existing green ammonia production process, is environmentally benign but not economical compared to MtA because of its high equipment and operating costs. The electrolyzer in the PtA process produces hydrogen and oxygen. Hydrogen can be supplied to the H-B process, and oxygen can be used for tri-reforming. The H_2O electrolysis process can use renewable electricity to produce NH_3 with substantially lower greenhouse gas emissions. ASU separates air into nitrogen and high purity oxygen (99.5%). Nitrogen can be supplied to the H-B process, and oxygen can be fed with air to the proposed tri-reformer. To overcome the drawbacks of these MtA and PtA processes, three new processes integrating green and blue processes with a tri-reformer are introduced in this study.

3-1. MtA Based on a Tri-reformer (MtA-TR)

Fig. 4 indicates the modification of the MtA process where the steam reformer, ATR, and furnace supplying heat to the steam reformer are replaced with the newly proposed tri-reformer. This modification leads to decreased fuel consumption as well as no emittance of CO_2 into air. No external heat is necessary for the tri-reformer because the energy required for endothermic reactions (steam and dry reforming) is supplied by an exothermic reaction (partial oxidation). The tri-reformer is followed by water gas shift

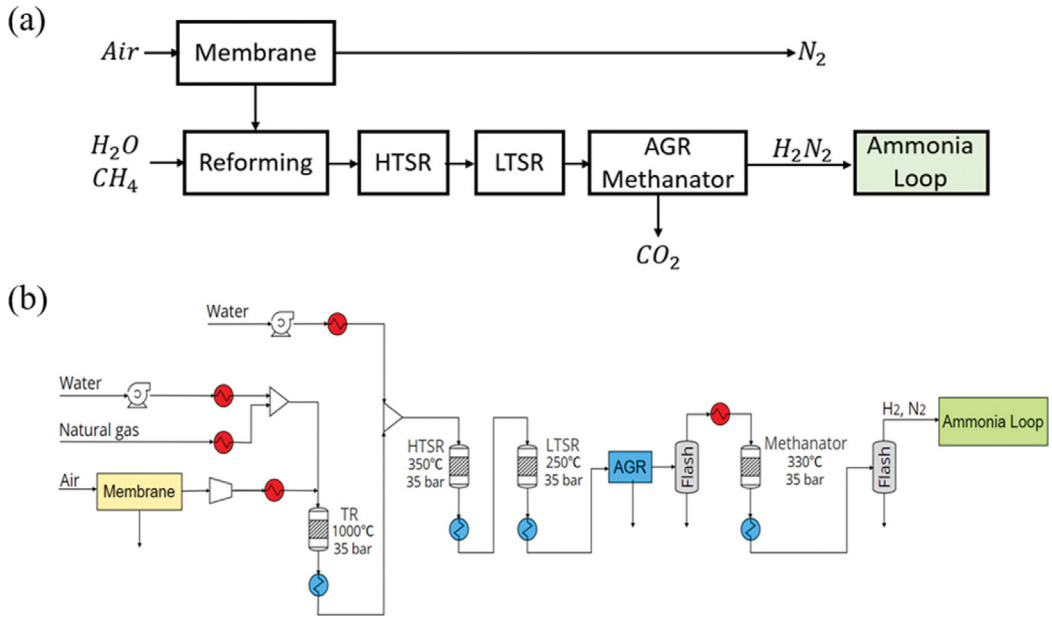

Fig. 4. MtA-TR (MtA process that involves introducing a tri-reformer instead of avoiding the use of primary and secondary reformers and furnaces): (a) process block diagram; (b) process flow diagram. The Rankine cycle (steam turbine network) is not shown in this figure but it is sized and optimized for maximizing heat recovery using pinch technology.

reactors, an AGR, and a methanator in the MtA. To achieve the necessary H_2/N_2 ratio of 3 for ammonia synthesis, a polymer membrane is utilized to control the O_2/N_2 ratio in the supplied air. The O_2 feeding rate is closely correlated with the H_2 production rate throughout the tri-reformer and hydrogen purification section. Similarly, the N_2 feeding rate must be adjusted in accordance with the H_2 production rate to achieve the appropriate mixture of H_2 and N_2 for ammonia synthesis. Although O_2 and N_2 are sourced from the ambient air, the O_2/N_2 ratio in the air may not align with the desired ratio for ammonia synthesis. Consequently, the ratio is modified using a polymer membrane. A mixture of H_2 and N_2 is compressed and fed to the ammonia synthesis process.

3-2. MtA Integrated with PtA (MtA-PtA)

Fig. 5 illustrates a new hybrid process that includes a tri-reformer and an electrolyzer. The use of a tri-reformer avoids the need for an energy-intensive steam reformer and furnace, leading to reduced CO_2 generation and methane consumption. Pure water is supplied to the electrolyzer where hydrogen and oxygen are produced. In the PtA process, hydrogen is used for the ammonia synthesis process, but oxygen is stored for sale. In the proposed process, oxygen is compressed and supplied to the tri-reformer with methane and air. The outlet stream of the tri-reformer has a composition with an H_2/N_2 ratio of 2-2.5 and passes through the water gas shift reaction, AGR, and methanator. The stream is then mixed with the hydrogen stream from the electrolyzer and fed to the ammonia synthesis process. N_2 for ammonia synthesis is obtained from the air supplied to the tri-reformer; oxygen is obtained from both the electrolyzer and ASU, and hydrogen is obtained from both the electrolyzer and blue hydrogen process.

In the thermoneutral tri-reformer, the following two reactions are dominant:

$$CH_4 + \frac{1}{2}O_2 \rightarrow CO + 2H_2,\ \Delta H^0_{298} = -35.6\ \text{KJ/mol} \quad (1)$$

$$CH_4 + H_2O \rightarrow CO + 3H_2,\ \Delta H^0_{298} = 206.3\ \text{kJ/mol} \quad (2)$$

The energy balance indicates that for each mole of CH_4 for steam reforming, approximately 5.8 moles of CH_4 are used for partial oxidation. The overall equation combining the two equations in energy balance is expressed as

$$6.8CH_4 + 2.9O_2 + H_2O \rightarrow 6.8CO + 14.6H_2 \quad (3)$$

A water gas shift reaction occurs in the subsequent processes, producing additional hydrogen.

$$6.8CO + 6.8H_2O \rightarrow 6.8CO_2 + 6.8H_2 \quad (4)$$

Component mole balances in the process:

$$N_2:\ F_{N_2} = 0.79F_{air} \quad (5)$$

$$O_2:\ 0.21F_{air} + 0.5F_{H_2} = 2.9 \quad (6)$$

$$H_2:\ 21.4 + F_{H_2} \quad (7)$$

Stoichiometric reactant mole ratio for ammonia synthesis:

$$N_2 : H_2 = 1 : 3 = 0.79F_{air} : 21.4 + F_{H_2} \quad (8)$$

For 6.8 moles of CH_4, 2.9 moles of O_2 should be supplied to the tri-reformer. Solving the equations gives 2.3 moles of H_2 produced from the electrolyzer (green hydrogen) and 21.4 moles of H_2 produced from the tri-reformer and subsequent processes (blue hydrogen). In summary, approximately 8% of total hydrogen is calculated to be green. However, the simulation gives a higher value of green hydrogen % (about 12%) mainly due to some loss of hydrogen during the production of blue hydrogen.

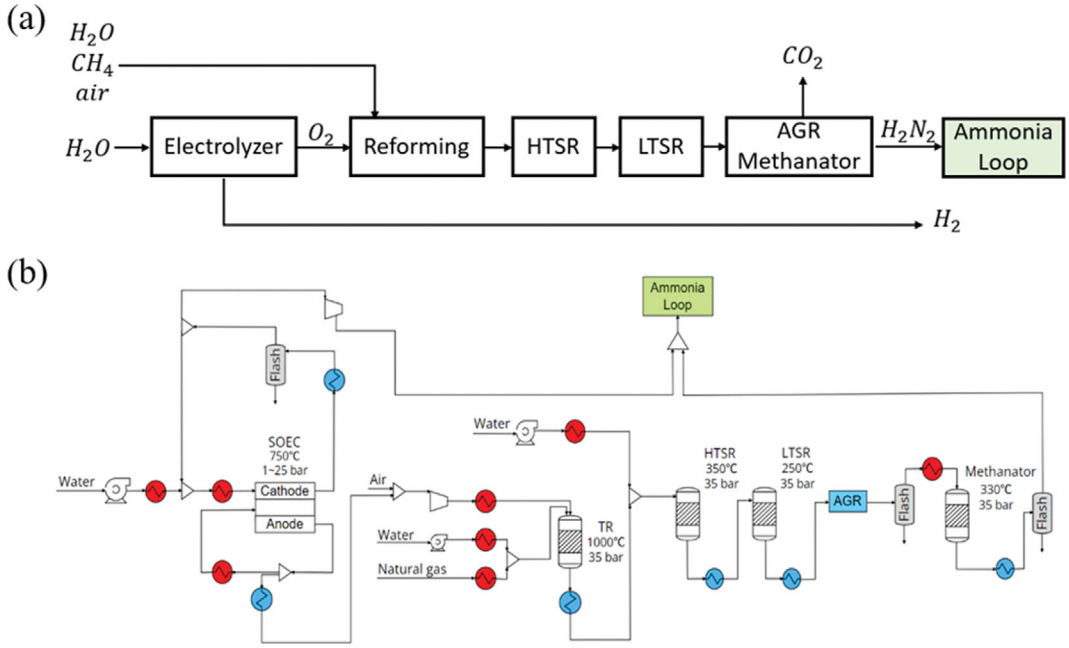

Fig. 5. MtA-PtA (oxygen from the electrolyzer is used for tri-reforming to produce H_2. H_2 from the electrolyzer and H_2 from the tri-reformer are mixed together and fed to the ammonia synthesis loop). The Rankine cycle (steam turbine network) is not shown in this figure but it is sized and optimized for maximizing heat recovery using pinch technology.

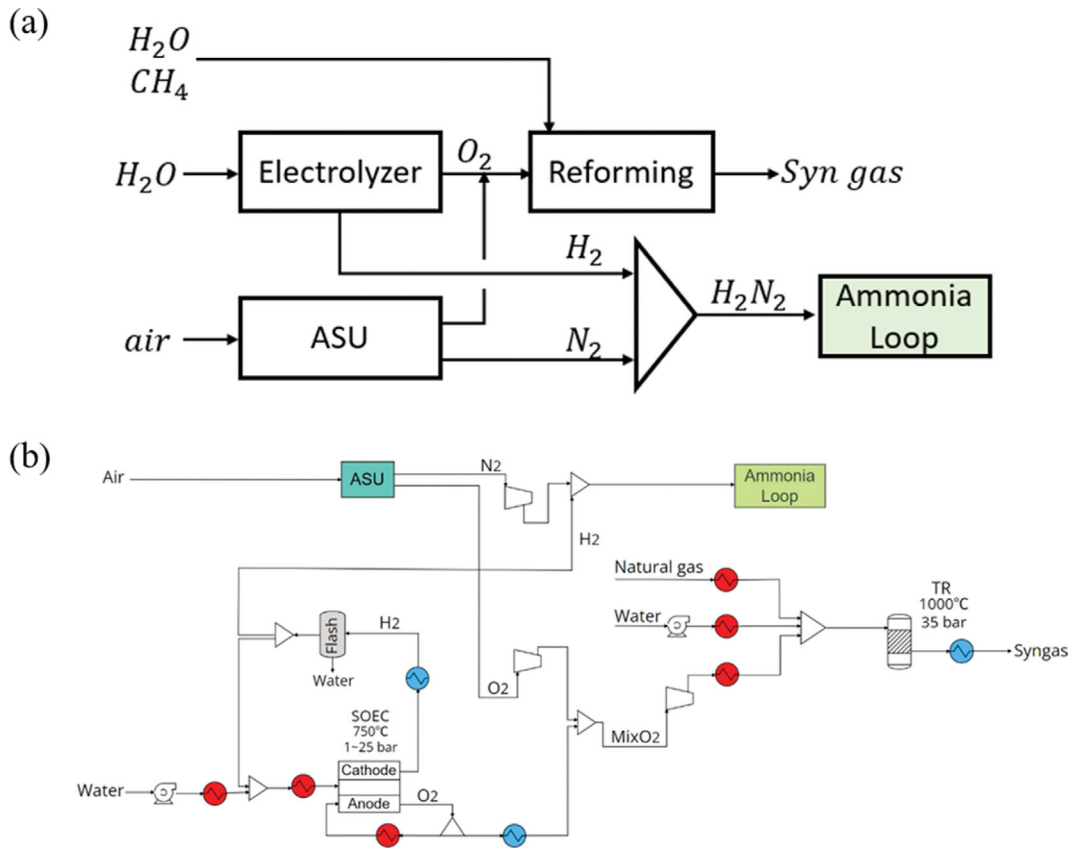

Fig. 6. PtA-MtS (oxygen from the electrolyzer and ASU is used for tri-reforming to produce syngas. H_2 from the electrolyzer and N_2 from the ASU are fed to the ammonia synthesis loop.): (a) process block diagram; (b) process flow diagram. The Rankine cycle (steam turbine network) is not shown in this figure but it is sized and optimized for maximizing heat recovery using pinch technology.

3-3. PtA Integrated with Methane-to-syngas (PtA-MtS)

Fig. 6 illustrates the hybrid process, which integrates the tri-reformer with a water electrolyzer and ASU. The process produces not only hydrogen for ammonia synthesis but also syngas for methanol production or the Fisher-Tropsch process. Here, the electrolyzer produces hydrogen for the ammonia synthesis process and oxygen for the tri-reformer. The ASU separates air into oxygen for the tri-reformer and nitrogen for the ammonia synthesis process. In this case, the water gas shift reaction, AGR, and methanator are not necessary in the process flow diagram because the final product of the tri-reformer is syngas, not hydrogen. The production capacities of the ASU and electrolyzer are determined by the H_2/N_2 ratio of 3 and the production rate of ammonia. Oxygen, as a product of the ASU and electrolyzer, and methane and water are supplied to the tri-reformer to produce syngas with an H_2/CO ratio of 2. Reactions in the tri-reformer occur at a pressure and temperature of 35 bar and 1,000 °C, respectively, and the syngas produced is cooled to 120 °C. This process also avoids the use of the primary steam reformer and furnace. This process offers several advantages, including the absence of CO_2 generation during the syngas production, opportunities of mass and heat integration between the PtA and MtS, and the production of syngas instead of solely oxygen. Assuming that the main reaction in the tri-reformer is partial oxidation, the production of one mole of green ammonia generates approximately 0.88 moles of oxygen, which can be utilized to produce approximately 5.3 moles of syngas.

PROCESS SIMULATION AND ECONOMIC MEASURES

Simulations for techno-economic analysis were performed using Aspen Plus. A design capacity of 50 kt/year for ammonia production was chosen, and the NH_3 purity was set to 99.5%. Reactor models for simulation are summarized in Table 1. Ammonia is commercially produced with a triple-bed adiabatic, quench cooled reactor. The reactor is modeled by the Rplug model in Aspen plus and the reaction kinetics are taken from [9]. The ammonia synthesis reaction kinetics can be expressed as the following:

$$r_{NH_3}=\frac{2f}{\rho_{cat}}\left(k_1\frac{P_{N_2}P_{H_2}^{1.5}}{P_{NH_3}}-k_{-1}\frac{P_{NH_3}}{P_{H_2}^{1.5}}\right) \quad \text{(kmol NH}^3\text{/kg cat h)} \tag{9}$$

$$k_1=1.79\times10^{4}e^{-87{,}090/RT} \tag{10}$$

$$k_{-1}=2.75\times10^{16}e^{-198{,}464/RT} \tag{11}$$

where P is the partial pressure (bar), ρ_{cat} is bulk density of the catalyst (kg/m^3), f is the correcting factor (4.75), k_1 and k_{-1} are pre-exponential factors for the forward and reverse reactions, respectively.

The ammonia was separated from effluent of the ammonia synthesis reactor at the condition of −5 °C and 135 bar, which was maintained by a refrigeration unit. The amount of electricity required

Table 1. Reactor models and conditions

Reactor	Description
Steam reformer	1) Fixed bed reactor of the Rplug model
	2) Endothermic reaction at 35 bar, 800 °C for a Ni based catalyst
	3) Xu and Froment reaction model [20]
Autothermal reformer	1) Fixed bed reactor of the Rplug model
	2) Adiabatic reaction at 35 bar, 1,000-1,100 °C for a Ni based catalyst
	3) Numaguchi and Kikuchi reaction model [21]
	4) Trimm and Lam reaction model [22]
Tri-reformer	1) Fixed bed reactor of the Rplug model
	2) Adiabatic reaction at 35 bar, 800-1,000 °C for a Ni based catalyst
	3) Xu and Froment reaction model [20]
	4) Trimm and Lam reaction model [21]
Water-gas shift reactor	1) Fixed bed reactor of the Rplug model
	2) HTSR: Isothermal reaction at 35 bar, 350 °C for a Fe based catalyst
	3) LTSR: Isothermal reaction at 35 bar, 250 °C for a Cu based catalyst
	4) Power law reaction model [23]
Methanator	1) Fixed bed reactor of the Rplug model
	2) Isothermal reaction at 35 bar, 330 °C for a Ni based catalyst
Ammonia reactor	1) Three-bed reactor of the Rplug model
	2) Exothermic reaction of 140-200 bar, 400-450 °C for an iron oxide based catalyst
	3) Power law reaction model [24]

Table 2. Process model and conditions for ASU, AGR, and SOE [3]

Equipment	Description
ASU	1) Cryogenic ASU; black-box model considering only the electricity requirement (Aspen Separator model)
	2) Separation of oxygen purity 99.5% at atmospheric pressure
	3) 160 kWh/ton pure O_2 electricity consumption
AGR	1) Black-box model considering only the reboiler heat duty and the electricity consumption (Aspen Separator model)
	2) inlet and outlet temperature: 40 °C-box
	3) CO_2 capture with 99% purity
	4) Reboiler requires an energy of 3.3 MJ/kg
	5) Electricity required for the pump: 25 kJ/kg
	6) Amount of MEA needed: 1.5 kg MEA/ton
SOE	1) Aspen Rstoic reactor, Aspen Separator model
	2) Requires a high temperature stream (above 750 °C)
	3) Electricity demand: 42 kWh/kg H_2
	4) Renewable energy available

for the unit was calculated from the coefficient of performance (COP), taken as 2.14 for a two-stage R717 vapor compression system employed in ammonia synthesis [18]. The primary reformer furnace and recovery boiler were modeled using the RGibbs model in Aspen Plus. The other process models and their conditions for simulation are listed in Table 2. The ASU and AGR were modeled as separators in Aspen Plus with the key energy consumption estimated from the literature. All reaction and process conditions were chosen according to the actual industrial standards.

The capital expenditure (CAPEX) for the key components was estimated based on [19]. The investment costs for each component were calculated considering the capacity, operating pressure and material grade. The purchase cost of the equipment, operating at atmospheric pressure and made of carbon steel, C_p^0, can be obtained using the following equation:

$$\log_{10} C_p^0 = K_1 + K_2 \cdot \log_{10} A + K_3 \cdot (\log_{10} A)^2 \tag{12}$$

where A is the capacity or size parameter, K_1, K_2, and K_3 are parameters. One can estimate the bare module cost (C_{BM}) of the components by scaling from the base component and considering the effect of time on the cost as follows:

$$C_{BM} = C_{p,\,ref}^0 \cdot \left(\frac{A}{A_{ref}^0}\right)^m \cdot \left(\frac{I}{I_{ref}}\right) \tag{13}$$

Table 3. Parameters for estimating the purchase cost of major equipment [3,13,19,27,28]

Equipment	$C^0_{p,ref}$ (M$)	A^0_{ref}	Base year	m
ASU	29.5	432 ton/day O_2	2009	0.65
AGR	18.1	1,227 kmol/hr CO_2	2009	0.65
Steam Turbine	5.9	10.3 MW	2002	0.65
Refrigerator	0.8	1 MW	2007	0.65
SOE single stack*	2.36×10^{-3}			
Tri-reformer	Reactor vessel capital cost: 10 times normal vessel cost with diameter=1; $10\times17.640\times(D^{1.066})\times(L^{0.802})$ with diameter and length in meters [13]			

* The SOE stack is taken as around 2,000 €/stack with a life time of about 48,000 h [3]

Table 4. Data used for estimating the operating costs and revenues

Economic data	Value	Unit	Ref.
Plant lifetime	25	year	[3]
Interest rate	10	%/year	[27]
Annual ammonia production rate	50,000	ton/year	[28]
Annual operating hours	7,200	hours/year	[3]
Electricity price	73	$/MWh	[27]
Electricity price for renewable energy	35	$/MWh	[3]
Natural gas price	17.7	$/MWh	[29]
Ammonia price	613	$/ton	[30]
Membrane lifetime	5	year	[31]
Membrane price	16.4	$/ton N_2	[32]
Nitrogen price	50	$/ton	[3]
Oxygen price	177	$/ton	[33]
Carbon oxide price	30	$/ton	[34]
MEA price	1,250	$/ton	[35]
Syngas price	298	$/ton CO	[36]
Operator salary	52,900	$/year	[3]

Table 5. Economic data related to the catalysts

Reactor	Catalyst name	Value ($/kg)	Life time (year)	Ref.
Steam methane reformer	Ni	10	5	[37]
Autothermal reformer	Ni	15	7	[38]
Tri-reformer	Ni	15	9	[38]
Ammonia reactor	Iron oxide	23	14	[39,40]
HTSR	Fe	17.64	4	[33,38]
LTSR	Cu, Zn	21.36	4	[41]
Methanator	Ni	17.7	4	[34]

where $C^0_{p,ref}$ and A^0_{ref} are the base cost and capacity of the equipment, respectively, and m is the cost exponent ranging from 0.65 to 0.85. I and I_{ref} refer to the cost indices at the desired time and base time, respectively. The grass roots cost (C_{GR}) can be calculated based on the bare module cost as follows:

$$C_{GR}=C_{TM}+0.5C_{BM} \quad (14)$$

where the total module cost $C_{TM}=1.18C_{BM}$. Table 3 gives the parameters for estimating the major equipment costs. The operating cost consists of the costs of the operating labor, feed material, catalyst, and electricity. The cost of the operating labor was estimated by using a technique based on Turton et al. [19].

With CAPEX and OPEX, the ammonia production cost C_{NH_3} can be obtained as follows:

$$C_{NH_3}=\frac{C_{opt}+C_{dep}-C^{byp}_{rev}}{P_{NH_3}} \quad (15)$$

where P_{NH_3} is the annual ammonia production rate (ton/year), C^{byp}_{rev} is the byproduct revenues ($/year) from the sale of syngas, exported electricity, oxygen, and carbon dioxide, and C_{dep} is the deprecia-

tion cost ($/year).

$$C_{dep} = C_{inv} \times \frac{i \times (i+1)^n}{(i+1)^n - 1} \quad (16)$$

where C_{inv} is the investment cost, i is the annual interest rate and n is the plant lifetime (year). The operating expenditure (OPEX) is calculated based on the assumptions given in Tables 4 and 5.

The payback time τ (year) can be obtained from

$$\tau = \frac{C_{inv}}{C_{rev}^{NH_3} - C_{rev}^{byp} - C_{opt}} \quad (17)$$

where C_{opt} is the operating cost including labor, fuel, catalyst and imported electricity and $C_{rev}^{NH_3}$ is the ammonia revenue ($/year). The carbon tax for CO_2 exhausted into the air and membrane replacement cost are considered in calculating the operating cost.

RESULTS AND DISCUSSION

1. System-level Heat Integration

Simulation of MtA, PtA and the proposed processes provides the mass and energy balances for the overall system, determining the heating and cooling duties for the system-level heat integra-

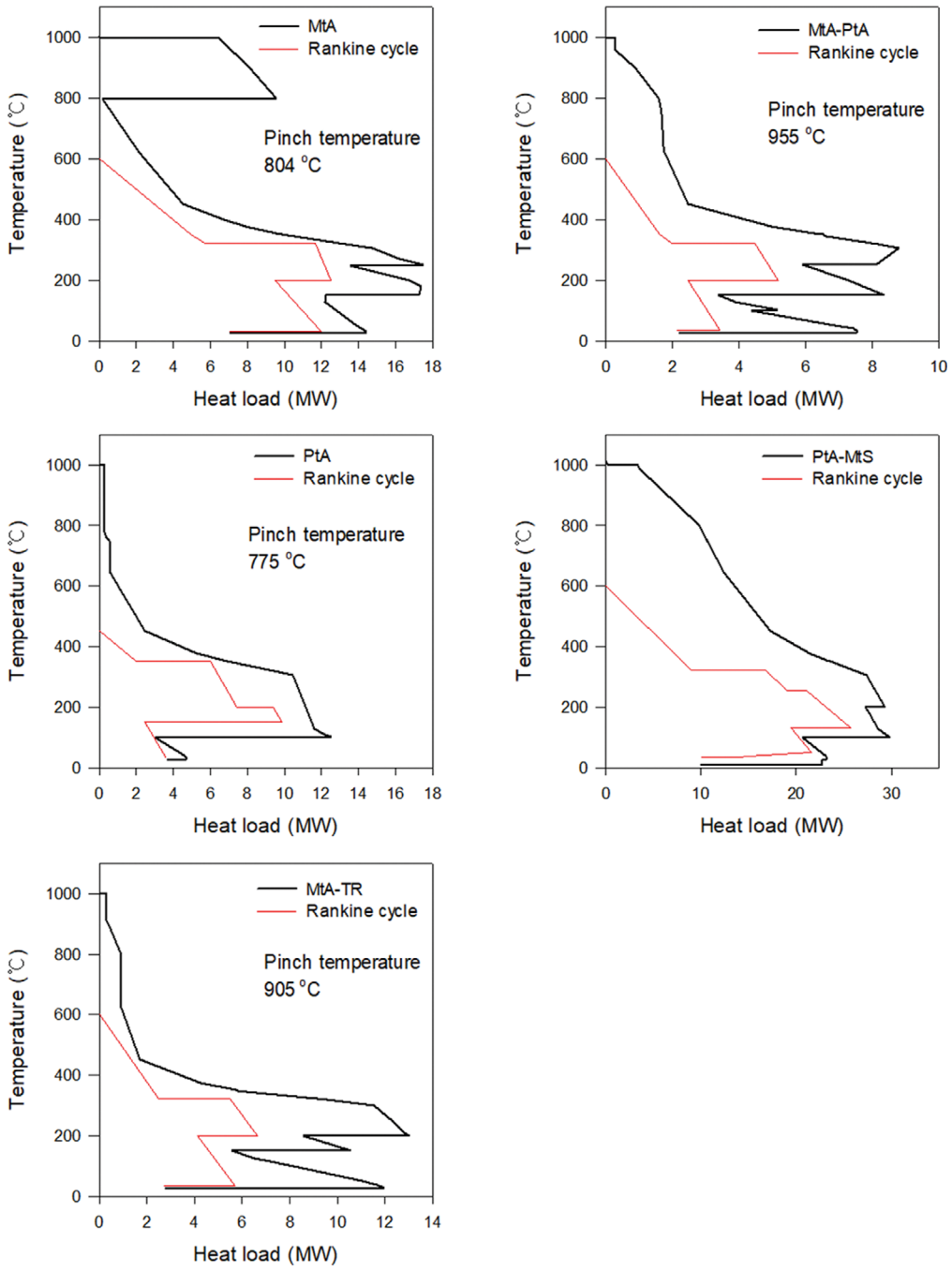

Fig. 7. Integrated grand composite curve including the Rankine cycle: (a) MtA; (b) PtA; (c) MtA-TR; (d) MtA-PtA; (e) PtA-MtS.

Table 6. Electricity consumption and generation

+Consumption/−Generation (MW)	MtA	PtA	MtA-TR	MtA-PtA	PtA-MtS
Electricity for the electrolyzer	-	+47	-	+5.6	+47
Other electricity consumption (compressor, refrigerator, AGR, ASU etc.)	+4.1	+4.4	+3.0	+3.2	+5.4
Electricity generated by the Rankine cycle	−6.8	−2.4	−2.4	−2.0	−9.5
Net electricity required	−2.7	+49	+0.6	+6.8	+42.9

tion. The steam turbine network (Rankine cycle) is implemented throughout the entire process, including the ammonia loop, to facilitate heat recovery and electricity generation in all cases. The Rankine cycle is a thermodynamic cycle that converts heat into mechanical energy which is usually used for generating electricity. Heat exchanger networks for the processes including steam turbine networks, are developed based on heat cascade calculations using the Aspen Energy Analyzer. The details can be found in [3,42,43]. The integrated grand composite curves for all the processes are given in Fig. 7. The grand composite curve is used to quantitatively assess the combined heat and power scheme. The steam cycle receives heat from the process (heat source) to produce power, and the exhaust steam from the steam turbine is then used for heating the process (heat sink). Table 6 provides the results of heat integration in terms of electricity for the conventional and proposed cases.

For the MtA case, the primary reformer furnace provides most of the heat requirement for the SMR. The heat from the high-temperature flue gas, secondary reformer and ammonia synthesis reactor is first used to generate the steam for the primary reformer. The grand composite curve indicates that there is a large potential for heat integration below the pinch. The large potential is used as a heat source for the Rankine steam cycle to produce electricity. The steam extraction after expansion in the steam turbine is mostly used for solvent generation in the AGR.

MtA has a large potential for heat integration, generating large amounts of electricity (6.8 MW). In contrast, MtA-TR and MtA-PtA have only small potential for heat integration. MtA-PtA combines blue ammonia process and the green ammonia process. However, the green fraction is approximately 12% of the total ammonia production, so the heat integration potential should be similar to that of MtA. This means that replacing the steam reformer, autothermal reformer and furnace with a tri-reformer leads to significant improvement in energy efficiency in MtA-TR and MtA-PtA. Electricity is partly utilized for the process, e.g., compressor, and the remaining electricity is exported. MtA can export a small amount of electricity, but MtA-PtA imports a small amount of electricity. MtA-TR can provide most of the electricity required for the process from the Rankine cycle.

The PtA case has a small potential for heat integration. PtA-MtS is basically PtA, and blue syngas is produced using oxygen from the electrolyzer and ASU. A large amount of oxygen is used, leading to a larger heat load for the syngas production line and the greatest integration potential with the Rankine cycle. A comparison of the electricity generated between PtA and PtA-MtS indicates that syngas production part in PtA-MtS has the largest potential for heat integration, generating a larger amount of electricity (9.5 MW). However, PtA and PtA-MtS involve the importing of a large amount of electricity due to the large amount of electricity required for the electrolyzer.

2. Economic Analysis

MtA suffers from fuel consumption in the furnace and the emission of CO_2 generated through fuel combustion into the atmosphere, posing energy and environmental problems. In particular, CO_2 generated from combustion leads to an increase in the carbon tax. In contrast, PtA is environmentally benign in that no CO_2 is generated and renewable energy can be used in the process. N_2 and H_2 for the synthesis of ammonia are produced from water electrolysis and the ASU. However, PtA has economic disadvantages such as the use of an expensive electrolyzer and the large power consumption of the electrolyzer. The price of the electrolyzer is estimated to be over 50% of the total capital cost and electricity cost for the electrolyzer reaches over 70% of the total operation cost. Figs. 8 and 9 provide the distribution of capital and operation costs for all the cases.

MtA-TR employs a tri-reformer instead of a steam reformer, furnace and autothermal reformer in the case of MtA. In the tri-reformer, partial oxidation is dominant, whereas in the reformers for MtA, the steam reforming reaction is dominant. Steam reforming produces more hydrogen than partial oxidation for a given methane feed. The tri-reformer requires a larger amount of methane and air than MtA to produce the same amount of hydrogen as for the case of MtA (Table 7). However, considering the amount of CO_2 generated from combustion in the furnace for the MtA process, this process generates a smaller amount of CO_2 than for the case of MtA (Table 8). By avoiding the use of a steam reformer and furnace and introducing a tri-reformer, one can reduce the

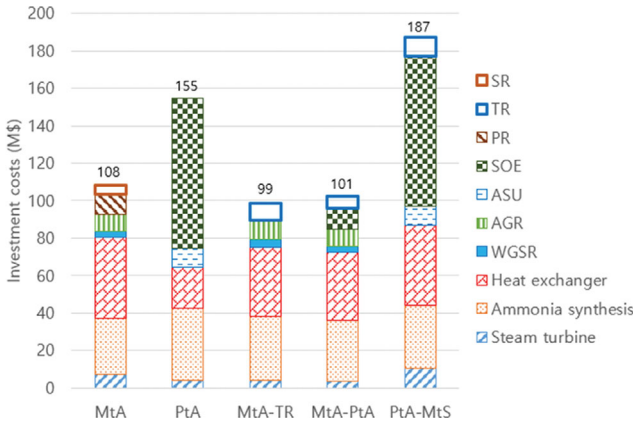

Fig. 8. The distribution of capital investment costs.

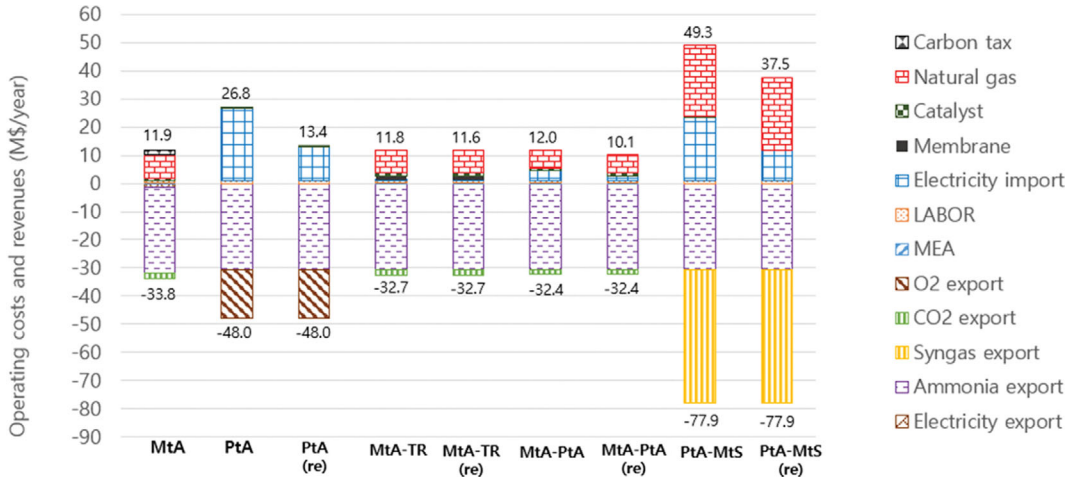

Fig. 9. The distribution of operating costs (positive value) and revenues (negative value) (re indicates renewable energy).

Table 7. Consumption of natural gas (NG)

kmol/hr	MtA	PtA	MtA-TR	MtA-PtA	PtA-MtS
NG for reforming reaction	202.4	-	244.8	200.9	785.2
NG for combustion	55.4	-	-	-	-
Total	258.1	-	244.8	200.9	785.2

Table 8. Generation of carbon dioxide

kmol/hr	MtA	PtA	MtA-TR	MtA-PtA	PtA-MtS
Amount of CO_2 captured	196.5	-	213.3	196.4	-
Amount of CO_2 emitted	57.5	-	-	-	-
Total	254	-	213.3	196.4	-

Table 9. Payback time (τ), ammonia production cost for all nine cases (* carbon tax 51 $/ton, ** carbon tax 100 $/ton, re indicates the use of renewable electricity)

	MtA	PtA	PtA (re)	MtA-TR	MtA-TR (re)	MtA-PtA	MtA-PtA (re)	PtA-MtS	PtA-MtS (re)
τ (year)	4.95* (5.38**)	7.31	4.47	4.74	4.71	4.95	4.53	6.53	4.63
C_{NH_3} ($/ton)	411.5 (446.0)	527.7	259.5	410.8	407.5	424.5	387.0	449.7	214.9

costs for the reactor and heat exchangers, leading to a large reduction in capital cost in MtA-TR and MtA-PtA. The capital cost of MtA-TR is estimated to be 9 M$ less than that of MtA and the operating cost for the process is slightly lower than that for MtA.

MtA-PtA avoids the use of a steam reformer and related equipment and introduces a tri-reformer and SOE for generating hydrogen. The capital cost for SOE (11.3 M$) is less than the cost reduction obtained by avoiding the use of a steam reformer and its related heat exchangers and introducing a tri-reformer. The capital cost of MtA-PtA (101 M$) is 6.5% lower than that of MtA. Electricity cost for MtA-PtA (5.6 MW) is higher than MtA due to the electricity required for operating an SOE. However, no carbon tax and reduced methane consumption are the advantages of the MtA-PtA process. Overall, the operating cost of the process (12.0 M$/year) is slightly higher than that for the case of MtA. However, if renewable energy is used, the operating cost is reduced to 10.1 M$/year.

PtA-MtS produces ammonia as well as syngas. The introduction of syngas production increases the capital cost for the process. The capital cost of PtA-MtS (187 M$) is higher than that of PtA (155 M$). The operating cost for PtA-MtS is mainly determined by the costs of methane gas and electricity. Table 7 indicates that a large amount of methane gas is required to produce syngas utilizing oxygen from an electrolyzer and ASU. The operating cost for PtA-MtS (49.3 M$/year) is much higher than that for PtA (26.8 M$/year). However, a higher syngas price than that of oxygen leads to a significantly high revenue (77.9 M$) for PtA-MtS compared

to PtA (48.0 M$). The net profit for PtA-MtS (28.6 M$) is higher than that for PtA (21.2 M$). The use of renewable electricity reduces the operating cost from 49.3 M$/year to 37.5 M$/year.

Table 9 shows the payback time and ammonia production costs for all cases. For MtA, a carbon tax of 51 $/ton is assumed to be a penalty for emitting carbon dioxide into the atmosphere. In this case, the inclusion of a carbon tax in the operation cost takes the role of increasing the payback time and ammonia production cost. Employing a future carbon tax of 100 $/ton makes MtA more unfavorable. MtA-TR has a lower payback time and ammonia production cost than MtA. MtA-PtA has a higher ammonia production cost than MtA, while the payback times for the two cases are the same. PtA-MtS has a lower payback time and ammonia production cost than PtA.

The economic viability of the processes largely depends on whether renewable energy is used for each process or not. When renewable energy is not used, MtA-TR is the most economical in terms of payback time and ammonia production cost. PtA and PtA-MtS are economically unfavorable because the payback times for the processes exceed six years. Both cases require large powers (49.0 MW for PtA, 42.9 MW for PtA-MtS), and the SOE equipment cost is also high. When renewable energy is used, PtA-MtS and PtA are the most economical cases. The payback times for both processes are below five years, and the ammonia production costs are significantly lower than that for the other cases. The utilization of renewable energy contributes to environmental sustainability by reducing the scope 2 emissions associated with processes reliant on conventional power purchased from external sources. However, the use of renewable energy has a significant problem: power intermittency. The intermittency of the power supply can cause an undesirable disruption in the ammonia synthesis loop. PtA and PtA-MtS are susceptible to the intermittency of renewable power supply. However, MtA-PtA is more tolerant to the intermittency. MtA-PtA has a small portion of PtA compared to MtA in ammonia synthesis and can change the portion in response to the intermittency in power supply.

3. Sensitivity Analysis

In Fig. 10, a sensitivity analysis is presented for all cases, considering changes in natural gas price, stack price, and electricity cost. Regarding payback time and ammonia production cost, PtA-MtS exhibits the highest sensitivity to fluctuations in natural gas price, followed by MtA, MtA-TR and MtA-PtA. This is primarily due to the larger quantity of natural gas utilized for syngas production in PtA-MtS compared to the other processes (MtA, MtA-PtA and process MtA-TR). PtA-MtS becomes the most advantageous when the natural gas price is below 16 $/MWh.

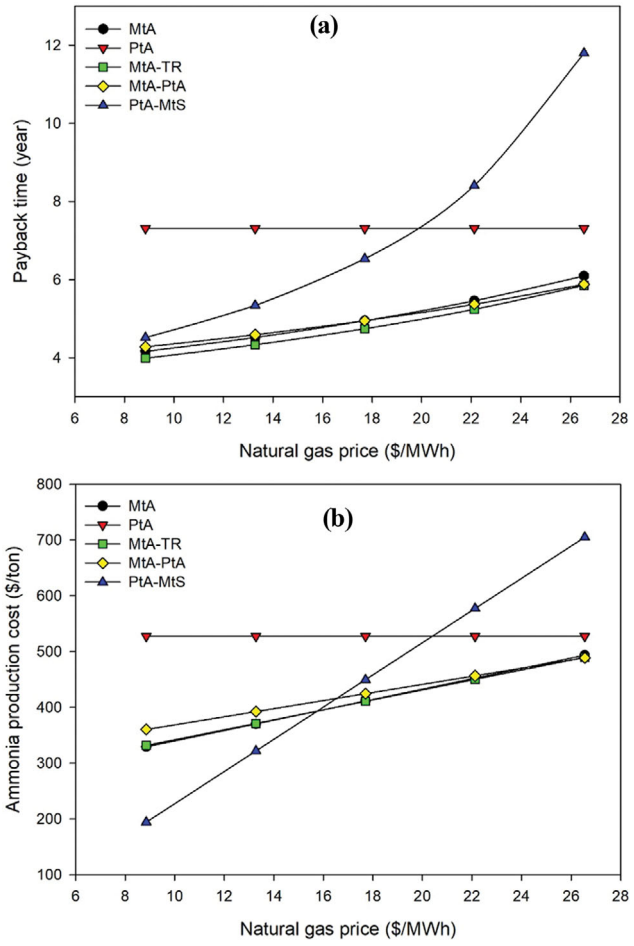

Fig. 10. Sensitivity of (a) payback time and (b) ammonia production cost to the natural gas price.

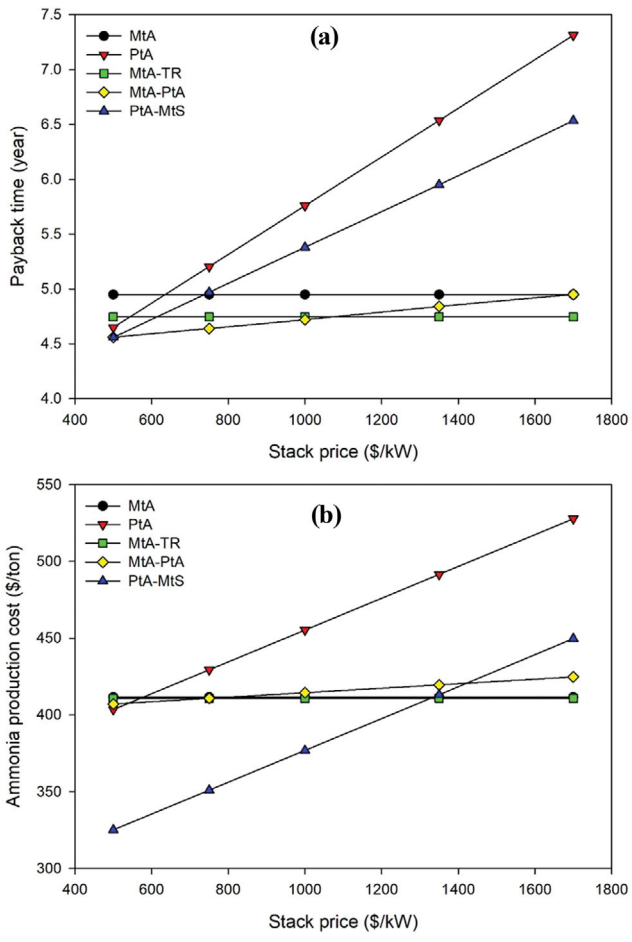

Fig. 11. Sensitivity of (a) payback time and (b) ammonia production cost to the stack price.

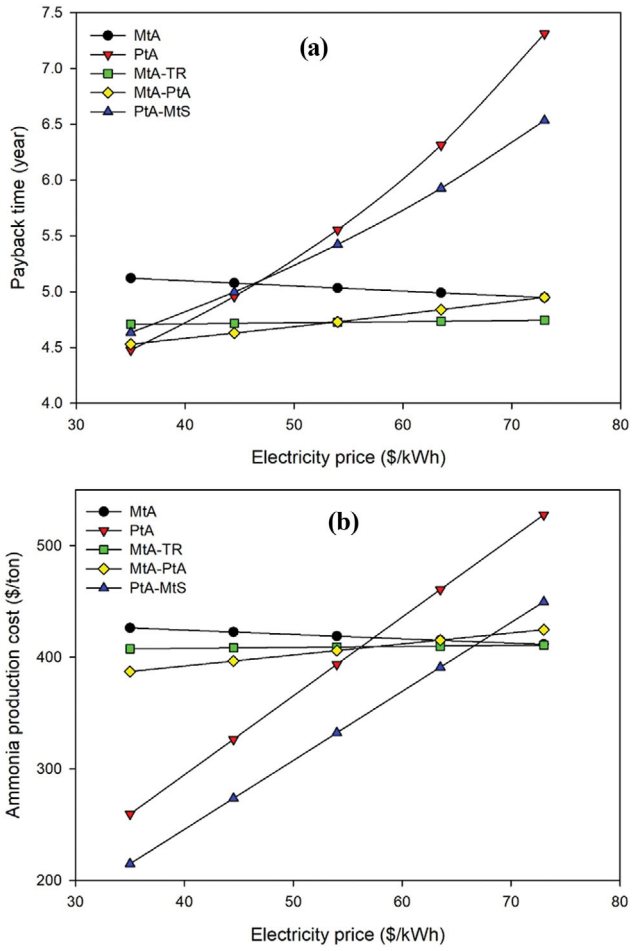

Fig. 12. Sensitivity of (a) payback time and (b) ammonia production cost to the electricity price.

Fig. 11 indicates that stack price has a great effect on the performance of PtA and PtA-MtS. Lower stack prices result in reduced capital costs for these two cases, leading to a substantial decrease in payback time. When the stack price is very low (below approximately 650 $/kW for PtA, 800 $/kW for PtA-MtS), PtA and PtA-MtS outperform MtA. Furthermore, in terms of ammonia production cost, PtA and PtA-MtS prove more favorable than MtA when the stack price is below 500 $/kW and 1,600 $/kW, respectively.

PtA and PtA-MtS are also highly sensitive to changes in electricity prices, affecting both payback time and ammonia production cost (Fig. 12). Comparing ammonia production costs, if the electricity price is lower than 68 $/kWh for PtA-MtS and 58 $/kWh for PtA, these two cases are more advantageous compared to the others. Additionally, concerning payback time, when the electricity price is very low, PtA and PtA-MtS can outperform other cases due to the high cost of the electrolyzer.

CONCLUSIONS

The conventional methane-to-ammonia (MtA) process suffers from high energy consumption and CO_2 emissions. Conversely, the power-to-ammonia (PtA) process, although environmentally benign, faces economic feasibility challenges due to high stack costs and electricity prices. In this study, we propose three new hybrid processes (MtA-Tr, MtA-PtA, PtA-MtS) that incorporate a tri-reformer and integrate the MtA and PtA processes, aiming to address both the economic and environmental issues. These processes were investigated from a techno-economic perspective and compared to the conventional MtA and PtA cases, as studied by Zhang et al. [3].

In the proposed processes, a tri-reformer replaces conventional reforming systems, including the primary steam reformer, secondary autothermal reformer, and furnace, simplifying the process and eliminating CO_2 emissions to the atmosphere. This simplification leads to a notable reduction in capital costs. MtA-Tr specifically applies this simplification to the MtA process. The tri-reformer also enables the effective utilization of the high-purity oxygen obtained from both the electrolyzer and air separation unit (ASU) within the PtA process. This integration becomes possible between the two processes, MtA and PtA. In MtA-PtA, the electrolyzer is introduced to produce green hydrogen, and the byproduct of the electrolyzer, oxygen, is utilized to produce blue hydrogen. In the PtA-MtS process, oxygen from the electrolyzer and ASU in PtA is utilized to produce syngas. These integrations provide additional opportunity to improve the economic performance of the processes.

Analysis of payback time and ammonia production costs reveals that MtA-Tr outperforms MtA and PtA-MtS outperforms PtA. MtA-Tr proves to be the most competitive when renewable electricity is not utilized, while PtA-MtS becomes the most competitive when renewable electricity is employed. These findings highlight the potential of integrating a tri-reformer and optimizing the utilization of oxygen from the PtA process to compensate for the drawbacks of both the conventional MtA and PtA cases.

REFERENCES

1. G. Soloveichik, *AIChE annual meeting*, Minneapolis, October 29-November 3 (2017).
2. R. Lan, J. Irvine and S. Tao, *Int. J. Hydrogen Energy*, **37**, 1482 (2012).
3. H. Zhang, L. Wang, J. V. Herleb, F. Maréchalc and U. Desideri, *Appl. Energy*, **259**, 114135 (2020).
4. P. H. Pfromm, *J. Renew. Sustain. Energy*, **9**, 034702 (2017).
5. J. Andersson and J. Lundgren, *Appl. Energy*, **130**, 484 (2014).
6. The Royal Society, Ammonia: zero-carbon fertiliser, fuel and energy store (2020).
7. D. Flórez-Orrego, F. Maréchal, S. Silvio de Oliveira Jr., *Energy Convers. Manage.*, **194**, 22 (2019).
8. L. Wang, M. Pérez-Fortes, H. Madi, S. Diethelm, J. V. Herleb and F. Maréchal, *Appl. Energy*, **211**, 1060 (2018).
9. H. Zhang, L. Wang, J. V. Herleb, F. Maréchalc and U. Desideri, *Energy*, **12**, 3742 (2019).
10. L. A. Wickramasinghe, T. Ogawa, R. R. Schrock and P. Müller, *J. Am. Chem. Soc.*, **139**, 9132 (2017).
11. O. Schmidt, A. Gambhir, I. Staffell, A. Hawkes, J. Nelson and S. Few, *Int. J. Hydrogen Energy*, **42**, 30470 (2017).
12. C. D. Demirhan, W. W. Tso, J. B. Powell and E. N. Pistikopoulos, *AIChE J.*, **65**, 7 (2019).
13. J. Jang and M. Han, *Int. J. Hydrogen Energy*, **47**, 9139 (2022).
14. A. T. Damanabi and F. Bahadori, *J. CO2 Util.*, **21**, 227 (2017).

15. A. Dwivedi, R. Gudi and P. Biswas, *J. CO2 Util.*, **24**, 376 (2018).
16. M. Sadeghi, M. Jafari, M. Yari and S. M. S. Mahmoudi, *J. CO2 Util.*, **25**, 283 (2018).
17. C. Song and W. Pan, *Catal. Today*, **98**, 463 (2004).
18. D. Flórez-Orrego and Jr. S. Oliveira, *Energy*, **141**, 2540 (2017).
19. R. Turton, R. C. Bailie, W. B. Whiting and J. A. Shaeiwitz, *Analysis, synthesis and design of chemical processes*, Pearson Education (2008).
20. J. Xu and G. F. Froment, *AIChE J.*, **35**, 88 (1989).
21. T. Numaguchi and K. Kikuchi, *Chem. Eng. Sci.*, **43**, 2295 (1988).
22. D. L. Trimm and C. W. Lam, *Chem. Eng. Sci.*, **35**, 1405 (1980).
23. H. F. Rase, *Case studies and design data*, New York, John Wiley and Sons (1977).
24. J. Morud and S. Skogestad, *AIChE J.*, **44**, 888 (1998).
25. A. Dutta and S. D. Phillips, Technical Report NREL (2009).
26. C. N. Hamelink, A. P. Faaij, H. D. Uil and H. Boerrigter, *Energy*, **29**, 1743 (2004).
27. Energy DG. Quarterly report on European electricity markets (2017).
28. Committee on Climate Change, Hydrogen in a low-carbon economy (2019).
29. Annual report 2017 of Gestore mercati energetici (2017).
30. S. Gary, P. Nick and S. Krista, *Farmdoc Daily*, **11**, 114 (2021).
31. C. Xi, L. Gongping and J. Wanqin, *Green Energy Environ.*, **6**, 176 (2021).
32. M. Bozorg, A. Bernardetta, V. Piccialli, S. Álvaro and C. Castel, *Chem. Eng. Sci.*, **207**, 1196 (2019).
33. J. Guilera, J. R. Morante and T. Andreu, *Convers. Manage.*, **162**, 218 (2018).
34. H. Naims, *Environ. Sci. Pollut. Res.*, **23**, 2226 (2016).
35. E. Oko, B. Zacchello, M. Wang and A. Fethi, *Greenhouse Gases Sci. Technol.*, **8**(4), 686 (2018).
36. R. Stephanie, S. Sumesh, P. Tom, W. Liang, Ø. Torbjørn and T. N. Alex, *Biotechnol. Biofuels*, **10**, 150 (2017).
37. https://www.alibaba.com.
38. R. M. Swanson, A. Platon, J. A. Satrio and R. C. Brown, *Fuel*, **89**, 11 (2010).
39. M. Akbari, A. O. Oyedun and A. Kumar, *Energy*, **151**, 133 (2018).
40. R. Bañares-Alcántara, G. D. Iii, M. Fiaschetti, P. Grünewald, J. M. Lopez and E. Tsang, *Analysis of islanded ammonia-based energy storage systems*, University of Oxford (2015).
41. E. C. D. Tan, M. Talmadge, D. Abhijit, J. Hensley, J. Schaidle and M. Biddy, *Technical Rep.*: NREL/TP-5100-62402 (2015).
42. F. Maréchal and B. Kalitventzeff, *Chem. Eng.*, **22**, 149 (1998).
43. F. Maréchal and B. Kalitventzeff, *Chem. Eng.*, **23**, 133 (1999).